29

Optoelectronic Feedback in Semiconductor Light Sources: Optimization of Network Components for Synchronization

Sora F. Abdalah[1], Marzena Ciszak[2], Francesco Marino[3], Kais Al-Naimee[4], Riccardo Meucci[5] and F. Tito Arecchi[6]
[1,2,4,5,6]*CNR-Isituto Nazionale di Ottica, Florence*
[1]*High Institute of Telecommunications and Post, Al Salihiya, Baghdad, Iraq*
[3,6]*Physics Department, University of Florence*
[4]*Physics Department, College of Science, University of Baghdad*
[1,2,3,4,5,6]*Italy*
[1,4]*Iraq*

1. Introduction

Synchronization phenomena have been the subject of intense studies since their first observation by Huygens in pendulum clocks. The subsequent discovery of deterministic chaos introduced a new kind of an oscillating system, a chaotic oscillator. In the late 1980s researchers turned their attention to the synchronization properties of chaotic systems (1–4), occurring when two, or more, chaotic oscillators are coupled, or, in case of the unidirectional synchronization, when a chaotic oscillator (master) drives another chaotic oscillator (slave). Despite their unpredictable nature, whose most remarkable feature is the exponential divergence of trajectories starting with infinitely close initial conditions, synchronization of chaotic systems is a phenomenon well established experimentally and reasonably understood theoretically.

The increasing interest in chaotic synchronization is motivated by its potential applications. Clear understanding of these phenomena and the dynamical mechanisms behind them opens new opportunities for applications in different fields of science. In biology, for instance, a challenging problem is to understand how a group of cells or functional units, each displaying complicated behavior, can interact with one another to produce a coherent response on a higher organizational level. In secure communications, a message can be hidden in the output of a chaotic system during transmission and can be recovered by using a copy of the original system, synchronized to the first (5). In this context, the investigation has been focused on chaotic optoelectonic devices.

Within the variety of dynamical regimes observed in semiconductor devices, chaotically spiking attractors play a special role. Typical time traces consist of large pulses separated by irregular time intervals in which the system displays small-amplitude chaotic oscillations. These erratic –though fully deterministic– sequences of pulses, mimic the dynamics experimentally observed in neurons (6) and many hypothesis have been done on their role in neural information processing (see (7) and references therein). Therefore, experiments

based on chaotically spiking units coupled in a network might be useful to simulate and model neuronal dynamics during a perceptual task. To this end, light-emitting diodes (LEDs) appear as ideal candidates since they allow the realization of a miniaturized chip of units optoelectronically coupled and an easier implementation in networks with various coupling topology.
In the following we report and characterize synchronization phenomena in such optoelectronic networks. In particular, we focus our attention on the experimental design, introducing a control bias voltage which allows to simplify the coupling scheme and to reduce the influence of small parameter mismatch in the network units.

2. Generation of chaotic optical pulses

The dynamics of LEDs can be typically described in terms of two coupled variables (intensity and carrier density) evolving with very different characteristic time-scales. The introduction of a third degree of freedom (and a third time scale) describing the AC-feedback loop, leads to a three-dimensional slow-fast system, displaying complicated bifurcation sequences arising from the multiple time-scale competition between optical intensity, carriers and the feedback nonlinear filter function. A similar scenario has been recently observed in semiconductor lasers with optoelectronic feedback (8). Here, we consider a closed-loop optical system, consisting of a LED with AC-coupled nonlinear optoelectronic feedback (see Fig. 1). The

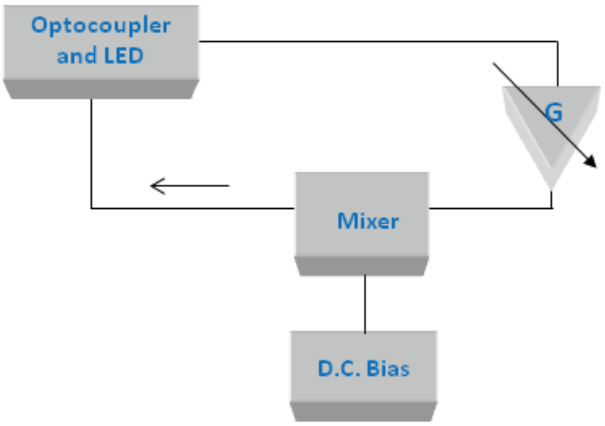

Fig. 1. Sketch of the experimental setup for LED.

output light is sent to a photodetector producing a current proportional to the optical intensity. The corresponding signal is sent to a variable gain amplifier characterized by a nonlinear transfer function of the form $f(w) = Aw/(1 + sw)$, where A is the amplifier gain and s a saturation coefficient, and then fed back to the injection current of the LED. The feedback strength is determined by the amplifier gain, while its high-pass frequency cut-off can be varied (between 1 Hz and 100 KHz) by means of a tunable high-pass filter. External signals or control bias can be added to the LED pumping current. Several of these units are eventually coupled through the detector photocurrent to form a network.
Fixed both the feedback gain and frequency cut-off and increasing the dc-pumping current, we observe the dynamical sequence shown in Fig. 2. In the upper panel, corresponding to the

lowest current, the detected optical power is stable. As the current is delicately increased a transition to a chaotically spiking regime is observed, where large intensity pulses are separated by irregular time intervals in which the system displays small-amplitude chaotic oscillations. As shown in Ref. (13) the chaotic spiking regime can be understood in terms of excitability of a chaotic attractor, where the small chaotic background spontaneously triggers excitable spikes in an erratic but deterministic sequence. The time-scale of these dynamics, much slower respect to typical carriers time scales ($\sim$ 1 ns), is fully determined by the high-pass filter in the feedback loop (8). Although similar to the well known Shilnikov homoclinic chaos observed in various physical systems (9–12), here the attractor structure is substantially different since an exact homoclinic connection to a saddle-focus does not occur. Further increase of the current makes the firing rate higher until a periodic regime is eventually reached (lower panel in Fig. 2). As the large pulses, these oscillations can be decomposed into a sequence of periods of slow motion, near extrema, separated by faster relaxations between them. This behavior (relaxation oscillations) is typical in multiple time-scales nonlinear systems. The same dynamical sequence can be obtained as the pumping current is kept constant and the amplifier gain is changed.

3. Synchronization in optical network

3.1 Symmetric coupling with control bias

Interactions between the constituents of physical or biological systems occur due to the existence of different types of connections: global, local, unidirectional or bidirectional. Besides of synchronization due to a direct coupling the systems may be synchronized by interaction via a common medium where the units interact through the exchange of some substances as occurs in many biological and chemical systems. In one dimension, the unidirectionally coupled systems (Fig.3 (a) and (c)) are defined in the following way:

$$\dot{\mathbf{x}}_i = \mathbf{f}(\mathbf{x}_i) + \mathbf{K}(\mathbf{x}_{i-1} - \mathbf{x}_i) \tag{1}$$

while bidirectionally (or nearest-neigbour) coupled systems (Fig.3 (b) and (d)) are defined as follows:

$$\dot{\mathbf{x}}_i = \mathbf{f}(\mathbf{x}_i) + \mathbf{K}((\mathbf{x}_{i-1} - \mathbf{x}_i) + (\mathbf{x}_{i+1} - \mathbf{x}_i)) \tag{2}$$

Depending on the boundary conditions the system form an one-dimensional array (open boundary conditions, see Fig. 3 (a) and (b)) or a ring (closed boundary conditions, see Fig. 3 (c) and (d)). The synchronization in the systems described in Eqs. 1 and 2 can occur for particular values of coupling parameters defined by matrix $\mathbf{K}$, when the difference between variables $\Delta x_{ij} = x_i - x_j$ vanishes. The difference variable Δx_{ij} multiplied by coefficient matrix $\mathbf{K}$ plays a role of a corrective signal which pushes the systems to the desired state of synchronization. In higher than one dimensions systems can be coupled globally (see Fig.3 (e)):

$$\dot{\mathbf{x}}_i = \mathbf{f}(\mathbf{x}_i) + \frac{\mathbf{K}}{N-1}\sum_{j\neq i}(\mathbf{x}_j - \mathbf{x}_i) \tag{3}$$

The coupling scheme defined in Eq. 3 can be replaced by a simpler one:

$$\dot{\mathbf{x}}_i \quad = \quad \mathbf{f}(\mathbf{x}_i) + \mathbf{K}_1\sum_{j<i}(\mathbf{x}_j - \mathbf{x}_i) + \mathbf{K}_2\sum_{j>i}(\mathbf{x}_j - \mathbf{x}_i + \mathbf{B}_i) \tag{4}$$

where $\mathbf{B}_i$ is a bias voltage, meanwhile $\mathbf{K}_1$ and $\mathbf{K}_2$ are the fixed-valued coupling matrices. The optimization aspects of the coupling scheme presented in Eq. 4 respect to the coupling

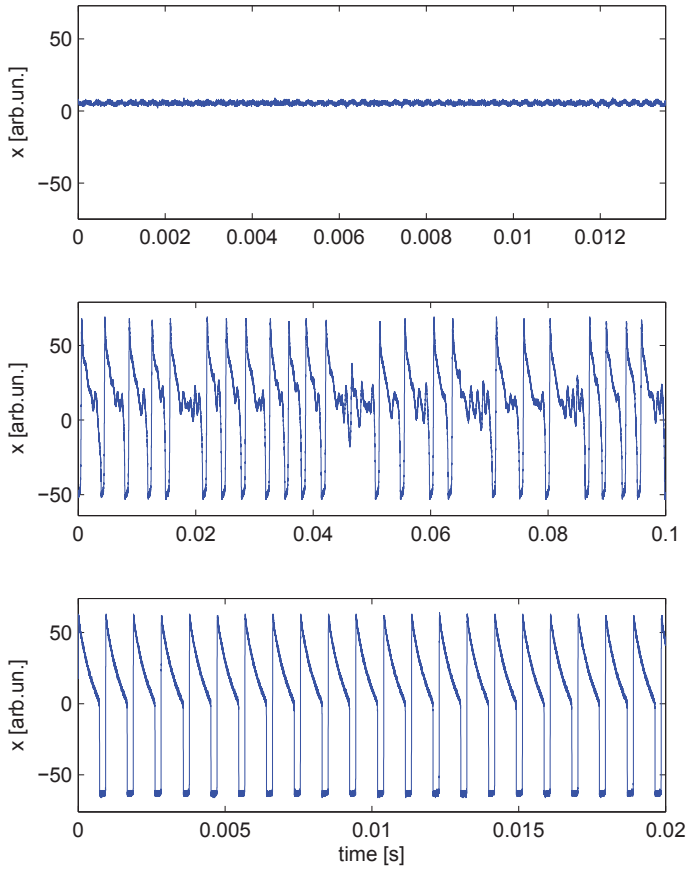

Fig. 2. Transition from a stationary steady state to chaotic spiking and eventually periodic self-oscillations as the dc-pumping current is varied in LED with optoelectronic feedback.

described in Eq.3 is explained below. Let us assume that the units are coupled only through a one system variable, i.e. a one observable in experiments, thus we consider $\mathbf{x}_k = x_k$. Then the total number of differential amplifiers used to get an input signal difference $\Delta x_{ji} = (x_j - x_i)$ which feeds the system x_i can be described by the binomial coefficient $E = 2\binom{N}{2} = \frac{N!}{(N-2)!}$, where N is the number of units in the network. It is however possible to decrease the number of elements by using the same signal difference Δx_{ji} as an input to a system x_j. In order to maintain the stability of synchronized solutions, in the second case, an additional bias voltage B_j is applied to the system x_j, so that it compensates the negative sign of the expression $-\Delta x_{ij}$ and allows to mimic an addition of the standard difference term Δx_{ij} required for the system x_j. For example, as shown in Fig. 4 in the case of $N = 4$, the number of elements reduces

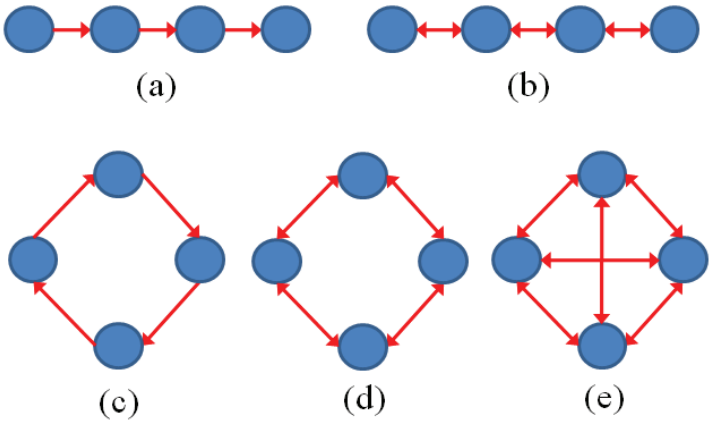

Fig. 3. Schematic presentation of different types of couplings (a) unidirectional, (b) bidirectional, (c) unidirectional in a ring, (d) bidirectional in a ring and (e) global.

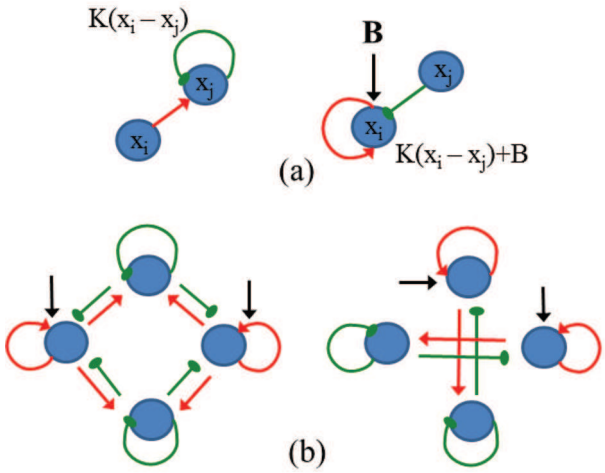

Fig. 4. Schematic presentation of the global coupling scheme with bias B: (a) compensation of the difference sign by B; (b) number of elements needed in the case of $N = 4$ units.

twice, from $E = 12$ to $E = 6$. The general value of elements E for N systems then becomes $E = \binom{N}{2}$.

Experimental results provided for 2 coupled systems, revealed that the transition to synchronization is not continuous as the control parameter, in our case the bias strength B, is varying. To describe quantitatively these abrupt changes we characterize the degree of order in the system by means of entropy S (see Ref. (14)). It is calculated from the distribution of the response times t_r in the time series. When the coupling is zero, this distribution is flat, i.e., the information on a site gives no information on the other ones. Increasing the coupling, we observe the birth of peaks for fixed time differences, due to the time correlation between

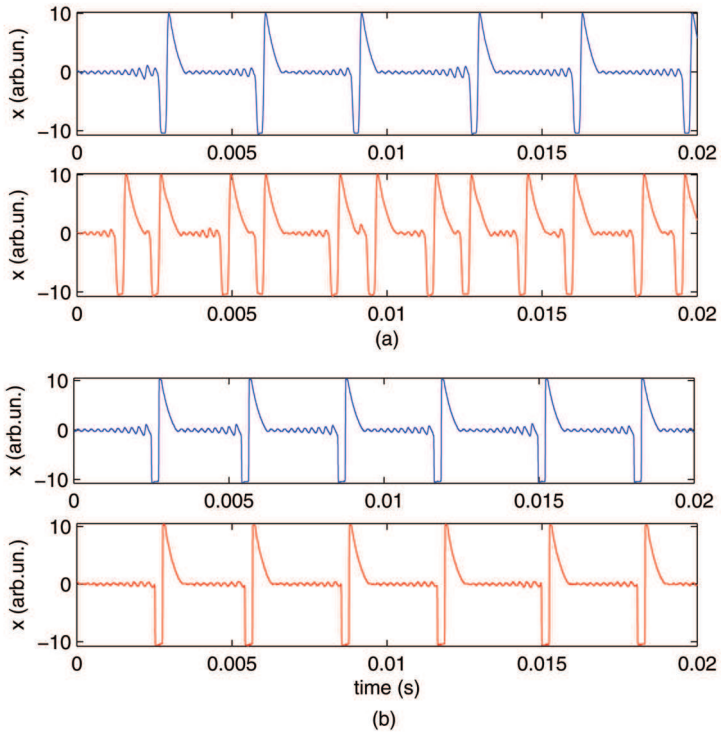

Fig. 5. Time series for 2 bidirectionally coupled LEDs in (a) desynchronized and (b) synchronized state.

spikes at adjacent sites. The entropy S is defined as follows:

$$S = -\sum_{t_r} p(t_r) \ln p(t_r) \tag{5}$$

where $p(t_r)$ is the probability distribution of t_r. The time series for two LED coupled with bias bidirectionally are shown in Fig. 5. Note, that in the case of N=2 systems, the implementation of Eq. 4 requires only one control bias B. The corresponding probability distributions are plotted in Fig. 6 (a). It can be seen that as the control bias is changing, the probability distribution becomes sharper giving rise to a low entropy values as reported in Fig. 6 (b).

3.2 Asymmetric coupling with control bias

The synchronization can be also obtained by constructing another types of couplings, not necessarily symmetric. One example, realized experimentally for 3 systems is based on a network with a doubly calculated difference $[x_3 - (x_2 - x_1)] + B$, which then feeds all 3 systems. Also in this case, the modulation of a control bias B enables to reach a synchronized state between all oscillators. Another type of asymmetric coupling has been applied to 6 LEDs. In this case it was defined as follows: $[(x_2 - x_1) + (x_4 - x_3) + (x_6 - x_5)] + B$, and again, used to feed all the six systems. The modulation of the control bias B enabled to reach synchronization between the systems as shown in Fig. 7. It is worth to note however, that the

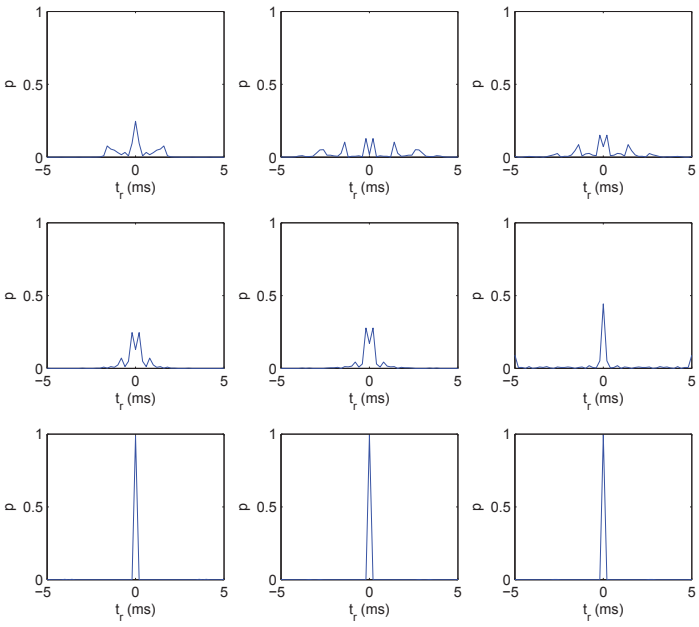

(a)

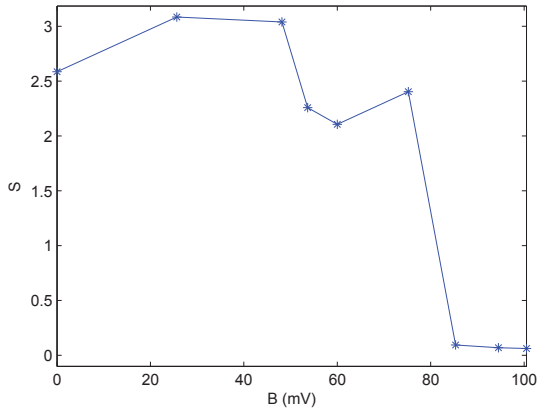

(b)

Fig. 6. (a) Distributions of the response times t_r and (b) corresponding entropy S versus bias B strength for two bidirectionally coupled LEDs.

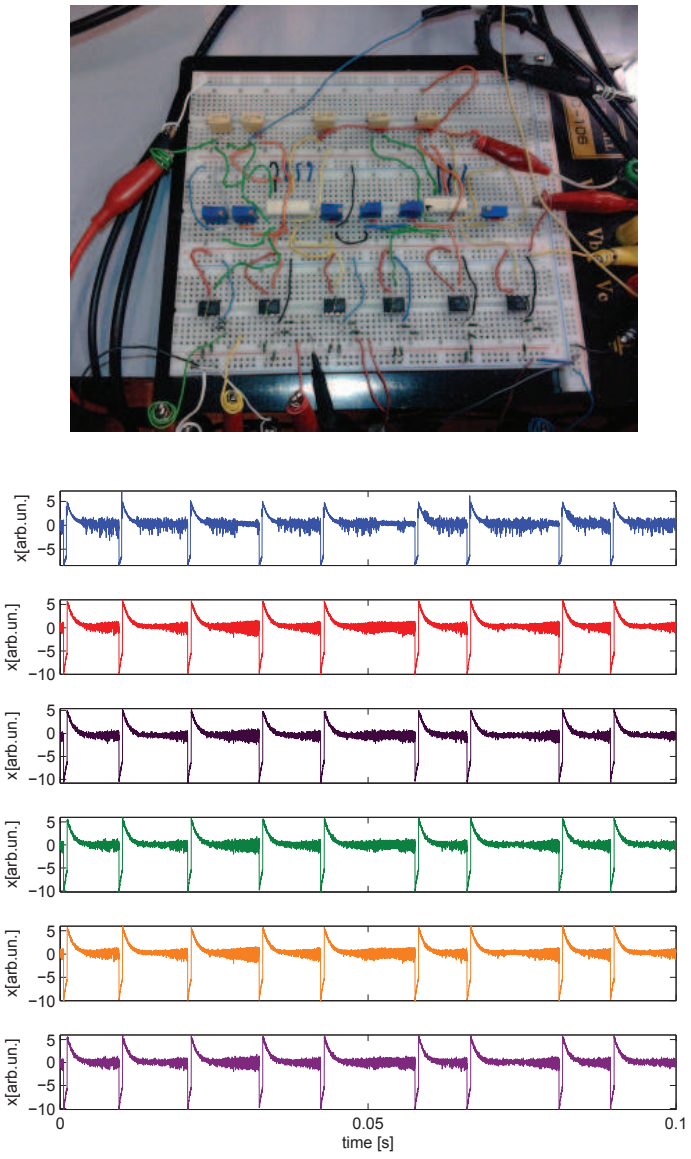

Fig. 7. Synchronization of six asymmetrically coupled chaotic LEDs.

synchronization occurs in high amplitude spikes, meanwhile the chaotic background of each oscillator is unsynchronized and follows its trajectory on its own chaotic attractor.

4. Conclusions

We presented the experimental results for the synchronization of chaotic optical network. The number of differential amplifiers has been reduced through adding of a bias voltage to the chaotic units. The adjustment of the single units dynamics, in order to reach a synchronized state within the all network, is a different kind of controlling the synchronization phenomenon as reported so far. This approach allows to control the parameter mismatch between the coupled units, what usually occurs in the experimental setups. Here, the collective interaction of the optical units has been reached through adjustment of the system states whereas the coupling strength is kept fixed. Moreover, we have realized experimental configurations for particular cases of asymmetric coupling in the case of three and six coupled oscillators. The synchronized state has been analyzed in terms of the probability distributions of the response times, measured between all interacting units. From the probability distributions the entropy has been evaluated what revealed the sharp decrease in its value as the bias voltage was modulated. An experimental observation of the transition to synchronization in an optical network is an important advance which can contribute not only to technological applications but also to experimental neuroscience. The latter problem, concerning the design of a miniaturized optical and functional neural network, will be the subject of our future study.

5. References

[1] Yamada, T. & Fujisaka, H. (1983). Stability Theory of Synchronized Motion in Coupled-Oscillator Systems. II. *Prog. Theor. Phys.* Vol. 70, pp. 1240-1248.
[2] Yamada, T. & Fujisaka, H. (1984). Stability Theory of Synchronized Motion in Coupled-Oscillator Systems. III. *Prog. Theor. Phys.* Vol. 72, pp. 885-894.
[3] Afraimovich, V. S.; Verichev, N. N. & Rabinovich, M. I. (1986). Stochastic synchronization of oscillations in dissipative systems. *Izv. Vys. Uch. Zav., Radiofizika* Vol. 29, pp. 1050Ű1060.
[4] Pecora, L. M. & Carroll T. L. (1990). Synchronization in chaotic systems. *Phys. Rev. Lett.* Vol. 64, pp. 821-824.
[5] Cuomo, K. M. & Oppenheim A. V. (1993). Circuit implementation of synchronized chaos with applications to communications. *Phys. Rev. Lett.* Vol. 71, pp. 65-68.
[6] Dafilis, M. P.; Liley, D. T. J. & Cadusch, P. J. (2001). Robust chaos in a model of the electroencephalogram: Implications for brain dynamics. *Chaos* Vol. 11, pp. 474-478.
[7] Arecchi, F. T. (2004). Chaotic neuron dynamics, synchronization and feature binding. *Physica A* Vol. 338, pp. 218Ű237.
[8] Al-Naimee, K.; Marino, F.; Ciszak, M.; Meucci, R.; Arecchi, F. T. (2009). Chaotic spiking and incomplete homoclinic scenarios in semiconductor lasers with optoelectronic feedback. *New J. Phys.* Vol. 11, pp. 073022.
[9] Marino, F.; Marin, F.; Balle, S. & Piro, O. (2007). Chaotically Spiking Canards in an Excitable System with 2D Inertial Fast Manifolds. *Phys. Rev. Lett.* Vol. 98, pp. 074104.
[10] Albahadily, F. N.; Ringland, J. & Schell, M. (1989). Mixed-mode oscillations in an electrochemical system. I. A Farey sequence which does not occur on a torus. *J. Chem. Phys.* Vol. 90, pp. 813.

[11] Petrov, V.; Scott, S. K. & Showalter, K. (1992). Mixed-mode oscillations in chemical systems. *J. Chem. Phys.* Vol. 97, pp. 6191-6198.
[12] Koper, M. T. M.; Gaspard, P. & Sluyters, J. H. (1992). Mixed-mode oscillations and incomplete homoclinic scenarios to a saddle focus in the indium/thiocyanate electrochemical oscillator. *J. Chem. Phys.* Vol. 97, pp. 8250.
[13] Al-Naimee, K.; Marino, F.; Ciszak, M.; Abdalah, S.F.; Meucci, R. & Arecchi F. T. (2010). Excitability of periodic and chaotic attractors in semiconductor lasers with optoelectronic feedback. *Eur. Phys. J. D* Vol. 58, pp. 187Ű189.
[14] Ciszak, M.; Montina, A. & Arecchi, F. T. (2008). Sharp versus smooth synchronization transition in locally coupled oscillators. *Phys. Rev. E* Vol. 78, pp. 016202.

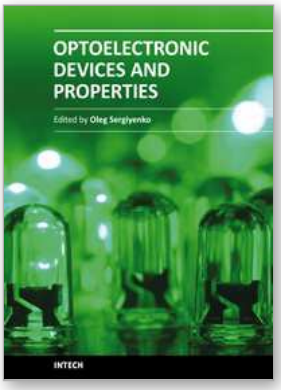

Optoelectronic Devices and Properties

Edited by Prof. Oleg Sergiyenko

ISBN 978-953-307-204-3
Hard cover, 660 pages
Publisher InTech
Published online 19, April, 2011
Published in print edition April, 2011

Optoelectronic devices impact many areas of society, from simple household appliances and multimedia systems to communications, computing, spatial scanning, optical monitoring, 3D measurements and medical instruments. This is the most complete book about optoelectromechanic systems and semiconductor optoelectronic devices; it provides an accessible, well-organized overview of optoelectronic devices and properties that emphasizes basic principles.

How to reference

In order to correctly reference this scholarly work, feel free to copy and paste the following:

Sora F. Abdalah, Marzena Ciszak, Francesco Marino, Kais Al-Naimee, Riccardo Meucci and F. Tito Arecchi (2011). Optoelectronic Feedback in Semiconductor Light Sources: Optimization of Network Components for Synchronization, Optoelectronic Devices and Properties, Prof. Oleg Sergiyenko (Ed.), ISBN: 978-953-307-204-3, InTech, Available from: http://www.intechopen.com/books/optoelectronic-devices-and-properties/optoelectronic-feedback-in-semiconductor-light-sources-optimization-of-network-components-for-synchr

INTECH
open science | open minds

InTech Europe
University Campus STeP Ri
Slavka Krautzeka 83/A
51000 Rijeka, Croatia
Phone: +385 (51) 770 447
Fax: +385 (51) 686 166
www.intechopen.com

InTech China
Unit 405, Office Block, Hotel Equatorial Shanghai
No.65, Yan An Road (West), Shanghai, 200040, China
中国上海市延安西路65号上海国际贵都大饭店办公楼405单元
Phone: +86-21-62489820
Fax: +86-21-62489821